Arch. Mech., 48, 4, pp. 779–788, Warszawa 1996

Changes of temperature during the simple shear test of stainless steel

S.P. GADAJ, W.K. NOWACKI and E.A. PIECZYSKA (WARSZAWA)

INVESTIGATION of the simple plane shear of stainless steel was carried out. The stress-strain curves and the distributions of infrared radiation for various shear rates have been registered. Temperature changes of the shearing paths were obtained on this ground. It was observed, that this temperature increases both with the increase of the deformation and the rate of shear. The capabilities of the used thermovision system allow us to notice the asymmetry of the thermal distribution of the shear paths caused by the macroscopic shear bands. Finally the results were compared with the results of numerical simulation, obtained for this kind of material deformed in adiabatic conditions.

1. Introduction

EXPERIMENTAL INVESTIGATIONS of the static simple shear are in general limited to the analysis of mechanical curves [1, 2, 3] and examination of the texture and microscopic pictures obtained for the material subjected to such deformation [3, 4, 5]. Theoretical approaches concern the analysis of the shear testing under the isothermic or adiabatic conditions [3, 6, 8]. In reality, the process of shear is accompanied by the heat emission and its almost immediate transmission to the surroundings, that significantly influences this process. This means, that the thermomechanical coupling occurs in nonadiabatic conditions. There are no papers on that problem published up to now, where the results of the investigations of the thermomechanical coupling during nonadiabatic static shear would be presented, though such investigations were undertaken during dynamic tests [7].

In this paper, the investigations of the static simple plane shear in nonadiabatic conditions have been carried out. Their goal was to obtain the mechanical curves as well as the temperature distributions in the shear areas. The results obtained enable us to present the temperature changes of the specimens subjected to the shear test with different rates of deformation, as well as to describe the macroscopic shear band, developing at higher deformations. Finally, experimental results were compared with the results of numerical simulations, calculated for the model of elasto-plastic material deformed in adiabatic conditions [8].

2. Description of experiment

The investigations were performed on the specimens of stainless steel 1H18N9T of composition: 0.076wt% C, 0.89wt% Mn, 0.45wt% Si, 0.02wt% P, 17.78wt% Cr, 9.24wt% Ni, 0.48wt% Ti. The samples of dimensions $30 \times 42.3 \times 0.5$ mm, cut out from the same sheet, were placed in a specially designed grip (Fig. 1), allowing

for replacing the compression by the simple shear. This grip was fitted in the Instron machine. Construction of this arrangement practically eliminates sliding of the specimen in the grip and ensures that the process of shear takes place on two parallel shear bands (paths) of the specimen, of 30 mm length and 3 mm width (Figs. 1 and 2). A change of temperature of the surface of these paths has been observed.

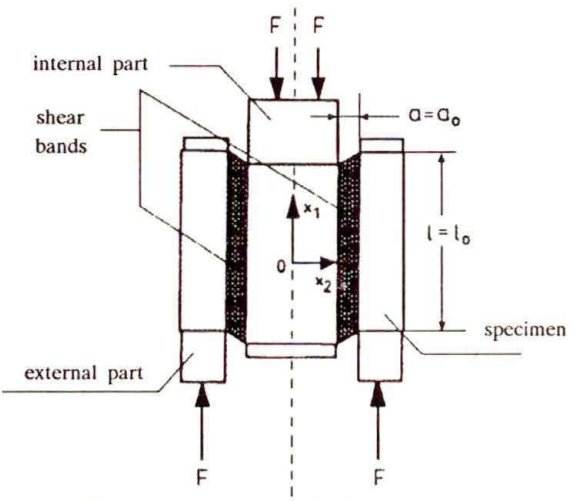

FIG. 1. Project of the device for fixing the specimens.

During the deformation, the load vs Instron's crosshead displacement, the load and this displacement vs time and the distribution of infrared radiation emitted by shear paths, were continuously registered. The infrared radiation was measured using the thermovision camera AGA 680 coupled with a system of data acquisition and conversion PTR WIN.

In order to secure higher and more homogeneous emissivity, the surface of the samples was blackened with carbon powder.

The shear tests were carried out with various, properly chosen rates of deformation: $2.77 \cdot 10^{-3}$, $5.55 \cdot 10^{-3}$, $11.1 \cdot 10^{-3}$ s^{-1}. These rates should be high enough in order to provide the sufficiently high temperature increments, measurable by the used thermovision set. The mean-square error of temperature evaluation was 0.3° C.

The system PTR WIN allows us to obtain the thermovision pictures with various precision. A thermovision camera scans the examined object collecting the infrared radiation from its surface. During 0.06 s the camera creates an image called frame. A thermal picture of the frame contains few details but, in spite of that, it can be very valuable. Short time of creation of these frames enables us to register more accurately the beginning of temperature changes of chosen areas of the object. An analysis of these temperature changes can be helpful for exact determination of the beginning of the process of shear or elongation. Four such

frames superimposed over each other create a thermal picture, obtained during 0.24 s. This thermal picture is a basis for analysing temperature distributions of the examined surface. Such distributions can be presented in different units depending on the chosen curve of calibration.

The PTR WIN software enables the user to obtain the following data:

- the temperature distribution on the surface of the examined body, with the chosen grade of discrimination: both black and white and coloured, stored on hard disc of a computer;
- the average temperature of the selected part of the picture, its mean-square error and the area of it;
- the real time temperature evaluation at several chosen points (up to 10);
- the temperature distribution along the line, arbitrarily chosen on the picture;
- the digital form of the obtained temperature distribution, which enables its further processing by other software.

3. Experimental results

The time, force and the crosshead displacement, registered during investigations, allow us to determine the stress and strain fields and to control the rate of shear. The stress tensor, defined in the coordinates shown in Fig. 1, has only 3 non-vanishing components: σ_{11}, σ_{22}, σ_{12} during simple shear. The single component of the tensor of deformation is $\gamma = \varepsilon_{12}$.

It was assumed that, in the case of simple plain shear in static conditions, there is no change in the cross-section: $S_E = \text{const}$ ($S_E = a_0 d$, where a_0 – width of the shear band, d – thickness of the specimen). Then the stress $\sigma_{12} = F/S_E$ and deformation $\gamma = \Delta l/a_0$, where Δl – displacement of the grips of the device holding the specimen (Fig. 1).

The distributions of intensity of the infrared radiation, recorded during investigation in digital form, allow us to reconstruct thermal pictures (thermograms) of the specimens. The maximal sensitivity of the system, conditioned by the 12 bit registration, is 0.01° C. In Fig. 2 an example of thermogram of the shear zones of specimen, deformed at the rate of $11.1 \cdot 10^{-3} s^{-1}$, and registered at the deformation $\gamma = 1.59$, is shown. A photograph of the undeformed specimen fixed in the grips of the holding device is given as well. The thermovision camera was focused on the shear zones since the grips are rather thick (15 mm). The coloured temperature scale is concerned with these shear zones only.

Because of the large mass of grips relative to the mass of specimen and because of the high heat conductivity of steel, there is a large temperature gradient in the direction perpendicular to the shear direction. The areas of maximum temperature are hence situated in the central part of the shear paths (along the direction of shear).

The occurence of the stress components σ_{11} and σ_{22} is caused by the condition $a = a_0 = \text{const}$ (the internal and external jaw of the grip move parallely, as shown in Fig. 1). The existence of free edges of specimen $x_1 = \pm l_0/2$, where the normal stress component must vanish, induces the heterogeneity of the strain field. However, it is assumed that this boundary region is small as compared to the length of the specimen. Theoretical considerations indicate that for $a_0/l_0 = 1/10$ ($l_0 = 30$ mm) this region covers almost 5% of specimen's length. An example of the strain field obtained numerically by the ABAQUS code for the steel 1H18N9T, under the assumption of elasto-plastic adiabatically deformed material at the strain level $\gamma = 0.322$, is shown in Fig. 3 A. Results of these calculations will be published in [9].

The disturbances of the stress and strain fields existing on free ends of the specimen during shear test are visible in the temperature distribution. The temperature of these areas is higher than in remaining part of the specimen. This is easily seen in the initial stage of the process. At higher deformations this effect is difficult to observe because of large temperature increments of the shear zones and due to high heat conductivity of this steel.

3.1. Temperature changes of the specimens subjected to various shear rates

The temperature changes of the shear paths for three deformation rates were investigated. Taking advantage of PTR WIN, 5 points were marked in the central part of the thermogram of one of these paths, where the temperature seemed to be homogeneous (Fig. 4, left picture). The coordinates of these points and their temperatures at the end of the process are given below. The graph of temperature evolution for these points during the shear time is shown on the right-hand side of Fig. 4.

The same approach was used for other rates of shear. The averaged values of temperature obtained this way are presented in Fig. 6 A as a function of deformation γ. The process of shear is accompanied by the increase in temperature. However, the temperature behaviour of the shearing specimen is a result of the heat emission and of its instantaneous flow to the grips; more particularly, that the used grips are solid, in comparison with the specimen. The temperature increments during shear test are not proportional to the stress of specimen. Looking at curves $\Delta T(\gamma)$ (Fig. 6 A) it can be noticed that for the deformation $\gamma \simeq 0.3$, an disorder in the monotonic temperature increase is observable, and an inflection point can be noticed. It can be related to the changes of the mechanisms of deformation at this stage of shear, however a full explanation of this phenomenon requires further investigations.

Figure 6 B presents the relations between the stress σ_{12} and the deformation γ, obtained for three shear rates. There are very small differences between these curves; the rate of deformation has no considerable influence on the mechanical characteristics of the material. Moreover, it is easy to notice that $\sigma_{12}(\gamma)$ curves are

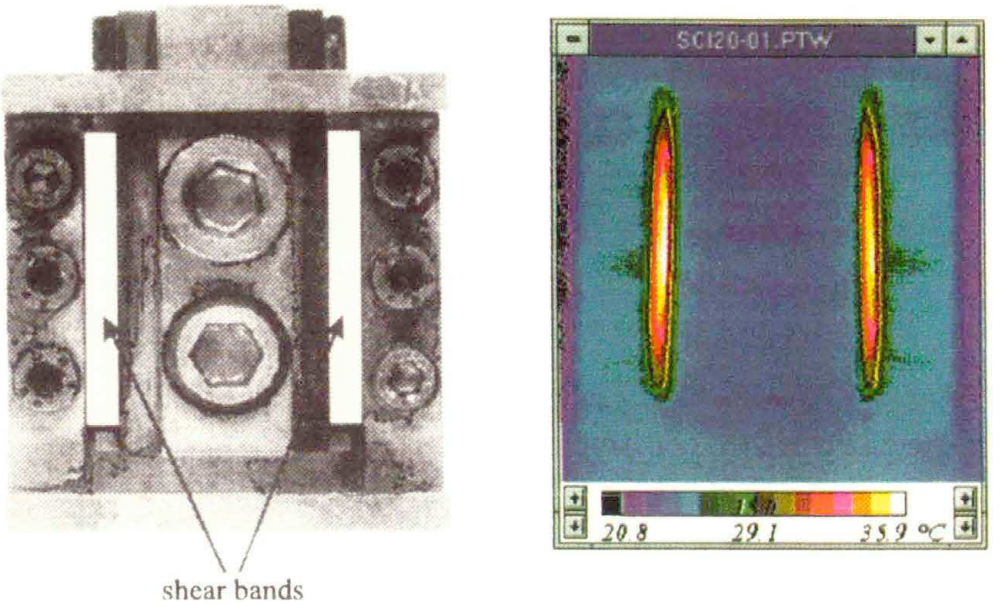

FIG. 2. Photograph of the specimen inserted in the holding device and a thermogram showing the temperature distribution in the sheared areas.

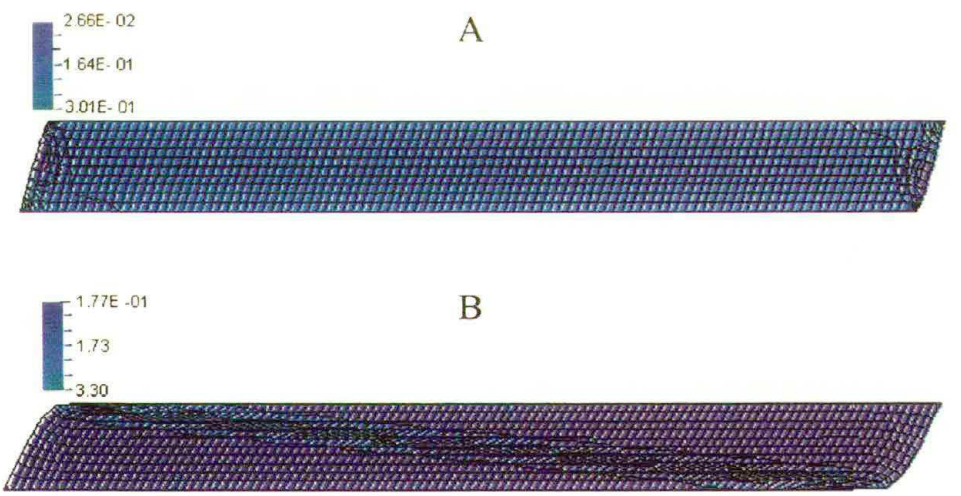

FIG. 3. (A) – heterogeneity of the field of deformation on the free edges of the sheared areas at $\gamma = 0.322$ and (B) – stress distribution in the shear areas at $\gamma = 1.11$; theoretical evaluation [9].

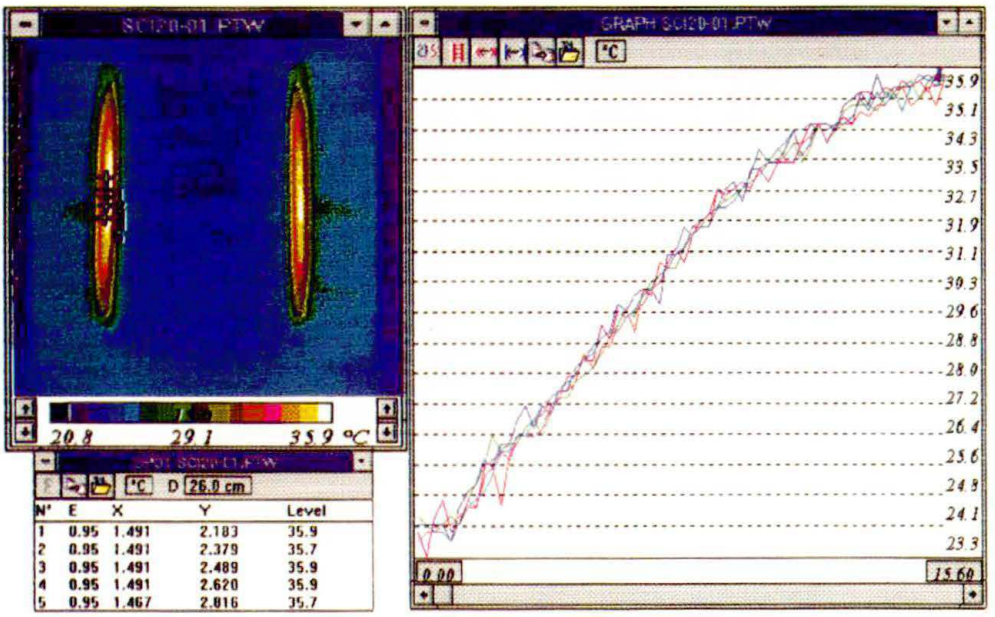

FIG. 4. A thermogram obtained during the shear test of 1H18N9T steel ($\gamma = 1.60$) and the temperature vs time for the chosen 5 points.

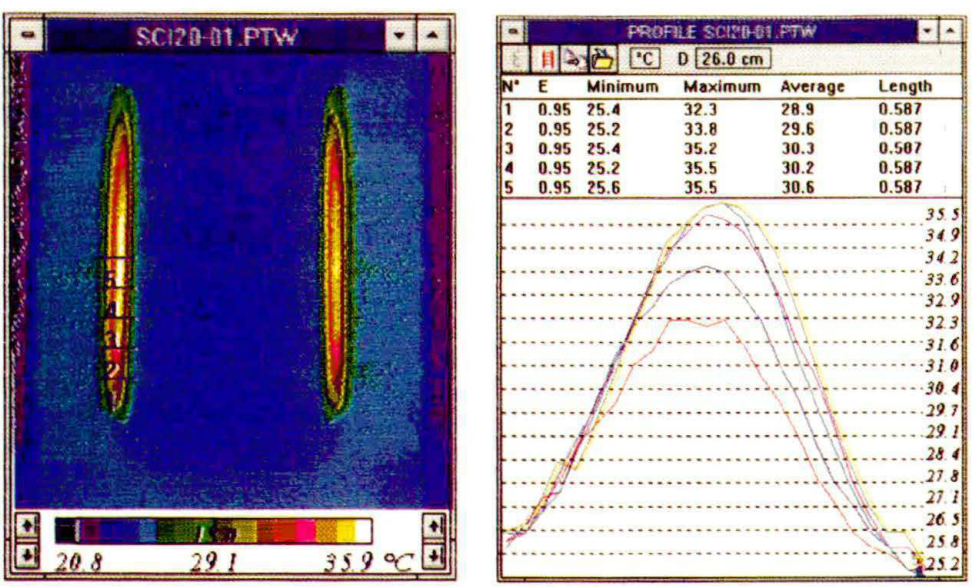

FIG. 5. A thermogram of the zones of shear with the 5 segments denoted. At right – the temperature distributions along these segments.

smooth up to $\gamma \simeq 70\%$. It gives evidence about the homogeneity of the process of shear in this stage of deformation. Then, the oscillating values of the stresses occurred, indicating the change of the character of deformation.

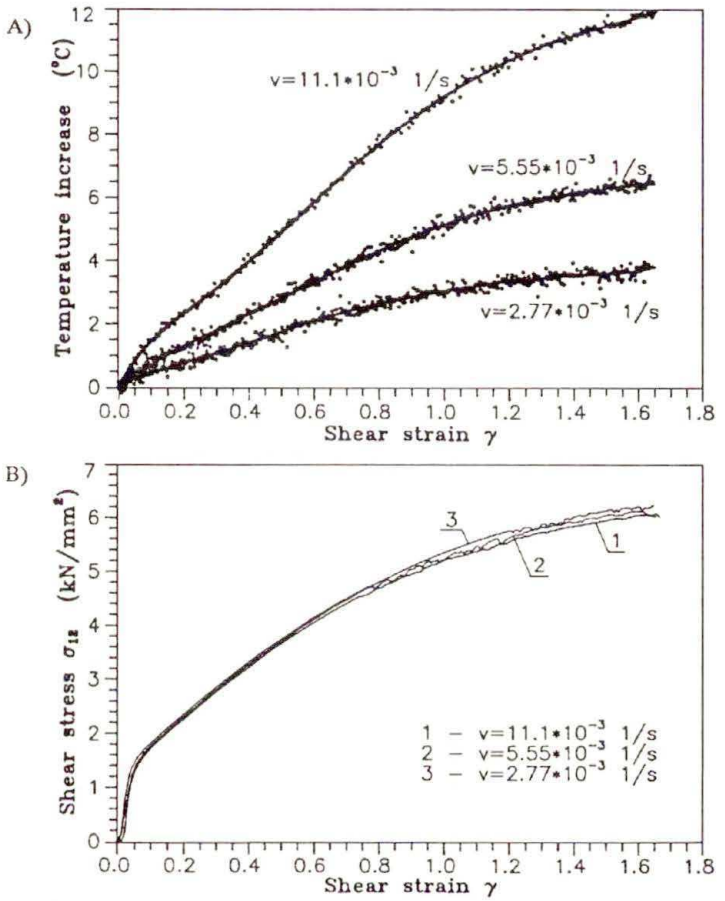

FIG. 6. Changes in temperature in the central part of the sheared path of the specimen made from 1H18N9T – (A), and the mechanical characteristics of this steel – (B); obtained at various rates of shear.

Summarizing the presented results (Fig. 6 A, B), it can be stated that there is a strong dependence of the temperature of shear paths on the shear rate, while the differences between the mechanical curves are insignificant.

3.2. Development of the macroscopic shear band

It follows from theoretical considerations that, during the simple shear test at deformations higher than $70 \div 80\%$, a localization of the deformation, named the macroscopic shear band, appears. The macroscopic shear band develops at a certain angle to the shear path. Figure 3 B presents a picture of this band for

$\gamma = 1.11$ shear deformation. The calculations were made for the elasto-plastic model of the body, under the assumption of combined isotropic-kinematic hardening and adiabatic process of deformation [9].

Suitable processing of thermal pictures recorded during the shear test indicates, that the phenomenon of localized deformation is noticeable also in nonadiabatic conditions, in which the experiment has been conducted. For that purpose the following approach was adopted.

On the thermograms obtained in non-homogeneous range of deformation ($\gamma \simeq 1.50$), 9 segments were chosen, intersecting the shear path perpendicular to the shear direction (Fig. 5). A coordinate x_2 of the beginning of each sector was the same (Figs. 1 and 5). Along these segments the distributions of temperature were determined. The determination of the temperature distributions was carried out in two approaches for each path, because the system PTR WIN enables us to obtain such distributions simultaneously for 5 segments only.

An example of the obtained thermograms with 5 marked segments and with the temperature distribution determined along them, is shown in Fig. 5. Ends of specimens are characterised by the inhomogeneous stress and strain state and, moreover, the temperature distribution is there influenced by other factors than in the remaining area. That is why these ends were omitted in the analysis of temperature distribution.

The procedure described above of obtaining the temperature distribution was applied to both shear paths. Subsequently, these distributions were approximated by the product of the exponential function and the Gauss function (Fig. 7). Since the exact scaling of the distances was very difficult, the coordinates of the points on the picture and the distances between them were given in relative units.

In agreement with the results obtained theoretically, the macroscopic shear bands of both paths obtained for the same specimen were directed towards each other (Figs. 1 and 3 B). Thus, the symmetrical superposition of the points indicating the temperature maxima in both paths and calculation of the mean value of the coordinate x_1 for these points (deviation of the temperature maximum from the shear direction) should eliminate a possible error caused by rotation of the paths relative to the shear direction.

The positions of points having maximum temperature were found for each specimen sheared at the rates $5.55 \cdot 10^{-3}\,s^{-1}$ and $11.1 \cdot 10^{-3}\,s^{-1}$. These positions were obtained for the deformations $\gamma = 0.63, 1.04, 1.59$. Small temperature increments accompanying the shear rate $2.77 \cdot 10^{-3}\,s^{-1}$ made it impossible to find the maximum of temperature.

The results of calculations obtained for extreme values of γ, where the macroscopic shear band occurs, are shown in Figs. 8 and 9. These are the mean values for both paths. The coordinate system was taken according to the Fig. 1; the x_1 axis – along the shear direction, and the x_2 axis – perpendicular to this direction. The position of maximum temperature, found for the segment lying in the middle of the path, was assumed as the origin of the coordinate system.

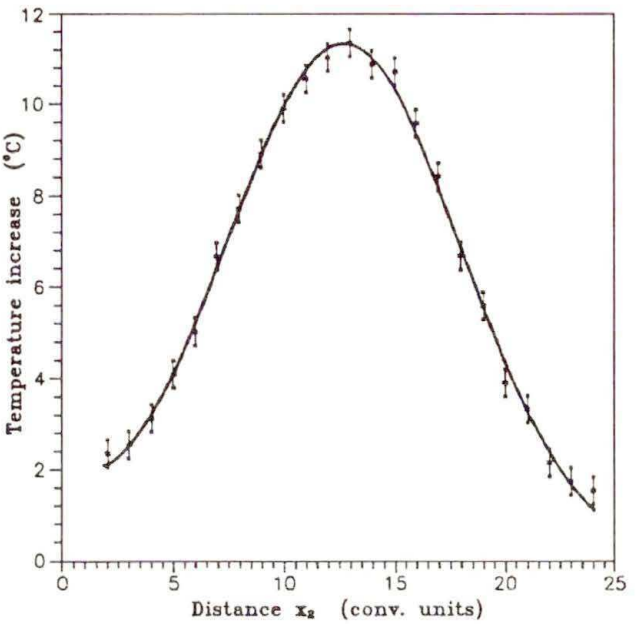

FIG. 7. Approximation of temperature distribution of the chosen sector by the product of the exponential and the Gauss functions. Accuracy of the measurement – 0.3° C.

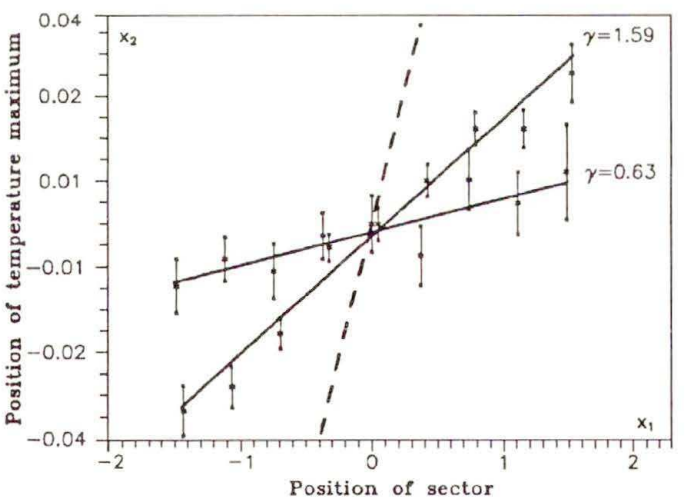

FIG. 8. Positions of maximum temperature in shear zones of the specimens at the strain rate $5.55 \cdot 10^{-3}\,s^{-1}$. Dashed line indicates the position of macroscopic shear band predicted by the theory (the direction of coordinate axes are given in Fig. 1).

For each point, the statistical error of the determined position of maximum temperature was calculated (Figs. 8, 9). Its value depends on the relative error of the temperature determination and decreases in accordance with a decrease

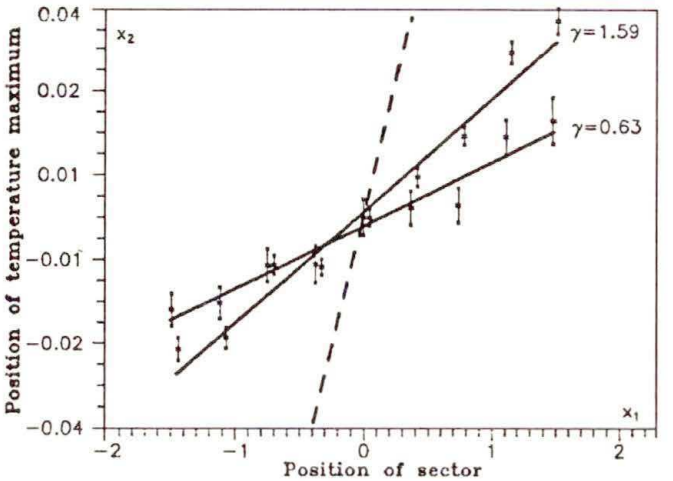

FIG. 9. Positions of maximum temperature in shear zones of the specimens at the strain rate $11.1 \cdot 10^{-3} s^{-1}$. The dashed line indicates the position of macroscopic shear band predicted by the theory (the direction of coordinate axes are given in Fig. 1).

in the temperature error. Other, nonstatistical errors of this determination were not taken into consideration.

The obtained values of the temperature maximum positions were approximated by the straight line $x_2 = mx_1 + n$, where m, n – the calculated coefficients. Results of this approximation were marked by solid lines, while the dashed line shows the position of the macroscopic shear band found from the theoretical calculations [8]. These results indicate that the line describing the position of the maximum temperature is not always situated in the middle of the shear path.

Table 1 shows the slopes, m, of the straight lines, obtained by the procedure described above, and the error, Δm, of its determination. The theoretical value of m is 0.1.

Table 1. The values of the slope m for different shear strain levels γ.

Shear rate	$\gamma = 0.63$		$\gamma = 1.04$		$\gamma = 1.59$	
$[s^{-1}]$	m	Δm	m	Δm	m	Δm
$5.55 \cdot 10^{-3}$	0.00624	0.00191	0.00979	0.00147	0.0220	0.0014
$11.1 \cdot 10^{-3}$	0.0120	0.0012	0.0136	0.0008	0.0212	0.0007

Results presented in Figs. 8, 9 and in Table 1 indicate that the slopes m increase accordingly to the rate of shear deformation.

The theoretical considerations [8, 9] were related to the shear rate $2.77 \cdot 10^{-3} s^{-1}$. At such rate, the position of the temperature maximum was impossible to determine in experiment. Besides that, in theoretical approach the macroscopic shear